RSC Advances

ROYAL SOCIETY OF CHEMISTRY

www.rsc.org/advances

Removal of disperse violet 28 from water using self-assembled organo-layered double hydroxides through a one-step process

Yan Li [*a], Hao-Yu Bi [b], Yong-Sheng Jin [a] and Xiao-Qin Shi [a]

[a] *Department of Chemistry, Changzhi University, Changzhi 046011 P R China*

[b] *Department of Biomedicine Engineering, Changzhi Medical College, Changzhi 046000 P R China*

[*] **To whom correspondence should be addressed**

E-mail: 15803455848@126.com

Tel: 0086-355-2178113 or 008615803455848

Abstract

A simple, one-step process including the self-assembly of organo-layered double hydroxides and removal of disperse dye simultaneously has been proposed. The one-step process is hopeful to be applied for dye effluents removal due to its low operation cost and simplified process compared with a traditional organo-layered double hydroxides process. Here, the self-assembly of organo-layered double hydroxides was realized by adding both raw layered double hydroxides and the anionic surfactant sodium dodecylsulfate into wastewater, and then the one-step process was applied to remove disperse violet 28 from dyeing wastewater. Results showed a higher removal efficiency of disperse violet 28 in this one-step process than in a traditional organo-layered double hydroxides process because cooperative removal and synergism between surfactant and disperse violet 28 in solution occurred to a large extent. The adsorption isotherm data could be described by the linear model, indicating a partitioning adsorption process. The adsorption kinetics was found to be well presented by the pseudo-second-order model, and the high activation energy (56.64 $kJ \cdot mol^{-1}$) indicated that the adsorption was mainly a chemical process.

Keywords: Layered double hydroxides; Anionic surfactant; Self-assembly; Adsorption; Disperse violet 28

1. Introduction

The treatment of dyeing wastewater from industries that produce and use dyes has been a key subject in recent years.[1] Synthetic dye stuffs are extensively used as coloring agents in some industries, such as textile, paper, leather, printing, plastic, pharmaceutical, and food.[2,3] Given the complex characteristics of dye-containing wastewater such as deep chromaticity, reducing sunlight penetration, low biodegradability, and complex composition, treatment by conventional processes is difficult.[4] Particularly, textile wastewaters present considerable resistance to biodegradation due to presence of the dyes which have a complex chemical structure and are resistant to light, heat and oxidation agents.[5] Although the majority of commercial textile dyes are water-soluble, some dyes present hydrophobic behavior, especially the disperse dyes that are used for dyeing polyester fabrics.[6] Disperse dyes are non-ionic aromatic compounds bearing azo or anthraquinone as a chromophore group, and some disperse dyes have also been shown to have a tendency to bioaccumulate.[7] Thus, appropriate treatments for dyeing wastewater, especially non-ionic dyeing wastewater, are important to identify and prevent environmental contamination. Several methods have been proposed to decolorize dyeing wastewater, namely, coagulation-flocculation, oxidation, electrochemical methods, adsorption, membrane filtration, and biological technology.[8-14] Among these techniques, adsorption is an efficient and economic process.[15] Recently, different low-cost adsorbents, such as sludge, rice husk, bentonite, fly ash, chitosan, and some agricultural by-products, have been used to remove color from dyeing wastewater.[16-20]

Layered double hydroxides (LDHs) are bidimensional solids with structural positive charge. LDHs consist of octahedral double hydroxyl layers that are isostructural to the brucite layer [$Mg(OH)_2$] with exposed positive surface charges and interlayer anions.[21] The general formula of LDHs can be represented as $[M_{1-x}^{2+}M_x^{3+}(OH)_2]^{x+}(A^{n-}_{x/n})^{x-}\cdot mH_2O$,[22] where M^{2+} and M^{3+} represent divalent and trivalent cations, respectively; x is equal to the ratio $M^{3+}/(M^{2+}+ M^{3+})$ and A^{n-} is an anion of valence n. LDHs are increasingly gaining attention as promising adsorbents because of their low cost, sheet-like structures, electrical properties, high specific surface area, and ion-exchange capacity.[23] LDHs, which have a hydrophilic surface, are suitable for the adsorption of anionic dyes but not non-ionic dyes, which are some of the most important dyes used in textile-dyeing industries.[24] Accordingly,

organo-LDH, synthesized from LDH and anionic surfactants, is used to adsorb non-ionic dyes.[1] Organo-LDH has good adsorption capability because the intercalation of anionic surfactants into LDH layers can change the surface of LDH from hydrophilic to hydrophobic.[1] The removal process using organo-LDH consists of two separate steps: the preparation of organo-LDH and the application of organo-LDH for non-ionic dye removal from wastewater by adsorption. Commonly used methods for the synthesis of organo-LDH include co-precipitation,[25] ion-exchange,[26] and regeneration[27] methods. However, organo-LDH is expensive to synthesize and more difficult to settle than LDH, which limits its application in wastewater treatment. Therefore, a simple one-step process involving the simultaneous self-assembly of organo-LDH and removal of non-ionic dyes in a system was proposed in the present study by adding raw LDH and an appropriate anionic surfactant to wastewater.

In addition, surfactants are always present as additives in wastewater produced by the textile industry.[28] Adsorption of non-ionic dyes accompanied by the self-assembly of organo-LDH could be directly conducted even if only LDH is used for wastewater treatment.

In this study, the self-assembly of organo-LDH [sodium dodecylsulfate (SDS)-LDH] and its adsorption behavior for the non-ionic dye disperse violet 28, which contain an anthraquinone chromophore, through a one-step process were tested. The aim was to reveal the removal mechanism of DV28 in this system by analyzing its adsorption isotherm and kinetics.

2. Materials and Methods

2.1 Materials

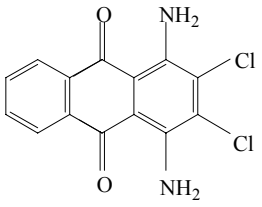

Fig. 1. Chemical structure of DV28.

Disperse violet 28 (1,4-diamino-2,3-dichloroanthraquinone; C.I. No. 61102; CAS No. 81-42-5; abbreviated as DV28; 0.90 mass fraction) was obtained from TCI (Shanghai, China) Development Co., Ltd. The chemical structure of DV28 is depicted in Fig. 1. DV28 stock solution was prepared by dissolving DV28 in deionized water to a concentration of 1.0 g·dm^{-3}. The necessary concentrations of

working solutions were obtained by successive dilution. Anionic surfactant SDS (0.99 mass fraction) was supplied by Sinopharm Chemical Reagent Co., Ltd. (Shanghai, China). All other reagents used were analytical grades.

2.2 Preparation of LDH

LDH was prepared by co-precipitation method. A mixed solution of $Mg(NO_3)_2 \cdot 6H_2O$ and $Al(NO_3)_3 \cdot 9H_2O$ was prepared in a molar ratio of 3:1. Afterwards, diluted $NH_3 \cdot H_2O$ was slowly dumped into the mixed solution to adjust the solution pH to about 9.5, which allowed precipitate formation. After aging for 1 h in the mother solution at room temperature, the precipitates were washed by pumping filtration with deionized water to remove residual $NH_3 \cdot H_2O$. Deionized water used was boiled and stored under nitrogen (N_2) gas before use. N_2 gas was also bubbled throughout the co-precipitation process to minimize errors caused by CO_2 in air. Finally, the filter cake was peptized at a constant temperature of 353 K in an oven for about 24 h to convert into LDH sol. The LDH sol was dried at 373 K to obtain the powder for use in later experiments.

2.3 Preparation of organo-LDH

For comparison, organo-LDH was prepared by ion-exchange method. Synthesized Mg-Al LDH was added to 0.1 $mol \cdot dm^{-3}$ SDS solution [100% theoretical anion-exchange capacity (TAEC) of LDH] with a solid-solution ratio of 1 g per 50 cm^3. The suspensions poured into 100 cm^3 plug-seal centrifuge tubes were shaken at a low speed on a reciprocal shaker for 24 h and centrifuged, and then the supernatant solution was decanted. The solid material was washed three times using deionized water and dried at 333 K to obtain organo-LDH powder. The ion-exchange reaction can be expressed by Eq. (1).

$$[Mg_{0.75}Al_{0.25}(OH)_2](NO_3)_{0.25} + 0.25\ CH_3(CH_2)_{11}OSO_3^- = [Mg_{0.75}Al_{0.25}(OH)_2](CH_3(CH_2)_{11}OSO_3)_{0.25} + 0.25\ NO_3^- \quad (1)$$

2.4 Characterization

Powered X-ray diffraction (PXRD) patterns of raw LDH (or organo-LDH) before and after adsorption were collected on a D/max-γB X-ray diffractometer (Rigaku, Japan) using Cu Kα radiation. All PXRD patterns were obtained from 2° to 70° at a scan speed of $4° \cdot min^{-1}$. Samples after adsorption were washed with deionized water three times and then air dried.

The chemical analyses of Mg and Al in samples were performed by atomic absorption spectrometry (Z-2000, Hitachi Co., Ltd., Japan) after dissolving the samples in concentrated HCl. The elemental compositions (C, H, N, S, and O) of the samples were determined using the dry combustion method with a Vario EL cube CHNSO elemental analyzer (Elementar, Germany). The chemical analysis results indicated that the formulae of raw LDH and organo-LDH were $[Mg_{0.69}Al_{0.24}(OH)_2](NO_3)_{0.24}\cdot 1.32H_2O$ and $[Mg_{0.68}Al_{0.24}(OH)_2](SDS)_{0.21}(NO_3)_{0.03}\cdot 2.26H_2O$, respectively.

The specific surface areas and total pore volumes of raw LDH and organo-LDH were measured at 77 K using N_2 as adsorbate with a sorptiometer (Autosorb-iQ, Quantachrome Co., U.S.) after vacuum degassing for 2 h at 333 K. The surface areas and total pore volumes were calculated based on the BET equation and Barrett-Joyner-Halenda analysis, respectively. The specific surface areas of raw LDH and organo-LDH were 44.72 and 5.26 $m^2\cdot g^{-1}$, and the total pore volumes were 0.273 and 0.036 $cm^3\cdot g^{-1}$, respectively.

2.5 Adsorption experiments

Batch adsorption experiments were carried out by mixing 25 cm^3 of DV28/SDS aqueous solution with 10 mg raw LDH as an adsorbent, denoted by raw LDH-SDS, at 200 rpm and 293 K for a certain time to ensure equilibrium. When equilibrium was achieved, the suspension was separated by centrifugation (12,000 rpm for 15 min), and the supernatant solution was analyzed for residual DV28 concentration, which was estimated using a UV-Vis spectrophotometer (U-3900, Hitachi Co., Ltd., Japan).

The effect of pH (5.5 to 10; adjusted with HCl or NaOH) on DV28 adsorption was studied at fixed SDS amount (100% TAEC) and raw LDH dose (10 mg) in 25 cm^3 of 50 $mg\cdot dm^{-3}$ DV28 aqueous solution at 293 K.

The effect of SDS amount (0 to 400% TAEC) on DV28 adsorption was studied at fixed raw LDH dose (10 mg) in 25 cm^3 of 50 $mg\cdot dm^{-3}$ DV28 aqueous solution at 293 K.

The effect of temperature (293 to 313 K) on DV28 adsorption was studied at a fixed raw LDH dose (10 mg) and SDS amount (100% TAEC) in 25 cm^3 of DV28 aqueous solution with different concentrations (5-50 $mg\cdot dm^{-3}$).

A preliminary kinetic investigation was performed over 24 h. Ten milligrams of raw LDH and SDS (100% TAEC) were added to 25 cm^3 of 50 $mg \cdot dm^{-3}$ DV28 aqueous solution at 293 (303 or 313) K.

For comparison, the adsorption kinetics and thermodynamics of organo-LDH for DV28 and the effect of pH on its adsorption at 293 K were investigated. The mass of raw LDH used to prepare organo-LDH was equivalent to that of raw LDH in the one-step process, i.e., the masses of raw LDHs in two adsorption processes were equal.

Each adsorption experiment was performed in triplicates using three independent samples, and the results were reproducible within ±3%.

3. Results and Discussion

3.1 Effect of pH on DV28 removal

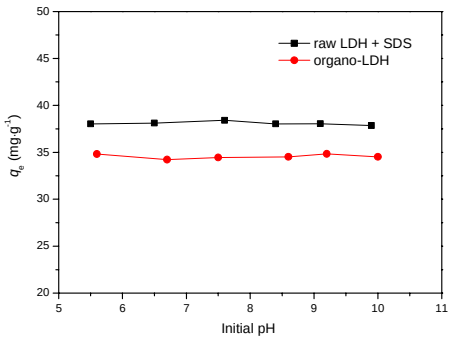

Fig. 2. Effect of initial pH on DV28 removal.

The pH value of the suspension was an important controlling parameter in the adsorption process. Fig. 2 shows the effect of initial pH (5.5-10) on DV28 removal by raw LDH-SDS and organo-LDH. As can be seen, solution pH was found to have negligible influence on DV28 removal in both raw LDH-SDS-DV28 and organo-LDH-DV28 systems. Since ~8.0 is the natural pH of the suspensions, therefore, further experiments were conducted without adjusting the pH.

3.2 Effect of SDS amount on DV28 removal

The influence of SDS amount on the adsorption capacity of raw LDH-SDS for DV28 is shown in Fig. 3. The effect of SDS on DV28 removal was prominent. DV28 adsorption almost linearly increased when the initial SDS concentration was <100% TAEC of LDH, and reached a peak, and then decreased when the initial SDS concentration was >160% TAEC of LDH. At low SDS concentrations, SDS was decisive for the enhancement of DV28 adsorption due to the interaction

between SDS and DV28, but DV28 adsorption was hindered by SDS at high SDS concentrations. SDS concentration at which DV28 adsorption began to decline was low, far from its CMC (~8 mmol·dm^{-3}).[29] The reasons for this phenomenon may be as follows. The electrostatic interaction between SDS and LDH surface or the hydrophobic interaction among SDS molecules enabled SDS to be continuously integrated in the LDH layer, leading to the closely packed structure of the LDH layer. The decrease in specific surface area (from 44.72 m^2·g^{-1} to 5.26 m^2·g^{-1}) and total pore volume (from 0.273 and 0.036 cm^3·g^{-1}) after intercalation may also be attributed to the pore blocking of aggregates and increased particle aggregation.[30] Therefore, steric hindrance effects ensued and hindered the close contact of DV28 to adsorption sites, thereby reducing DV28 adsorption. In addition, free SDS micelles will form and solubilize DV28 molecules if initial SDS concentration is larger than 8 mmol·dm^{-3}, and the amount of DV28 removed will decrease more.

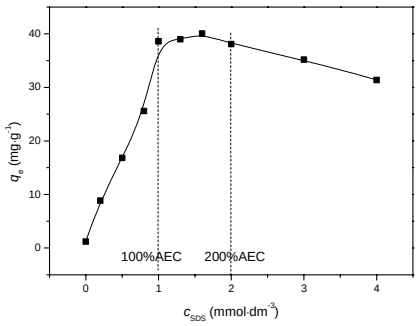

Fig. 3. Effect of SDS amount on the adsorption of DV28 on raw LDH-SDS.

3.3 Adsorption isotherms

The equilibrium isotherms are often used to describe experimental data of equilibrium adsorption. Fig. 4 shows the plots of adsorption isotherms of DV28 on raw LDH-SDS and organo-LDH at 293 K. As can be seen from Fig. 4, with increased initial concentration, the amount of DV28 adsorbed onto raw LDH-SDS increased to a greater extent than the traditional organo-LDH, i.e., raw LDH-SDS showed higher retention capacity for DV28 than the traditional organo-LDH.

It is important to establish the most appropriate correlation for the equilibrium curves for the design and operation of adsorption systems. The adsorption isotherms that are often used to describe the experimental data are Langmuir, Freundlich, Linear, Temkin, and Dubinin-Redushkevich isotherms.

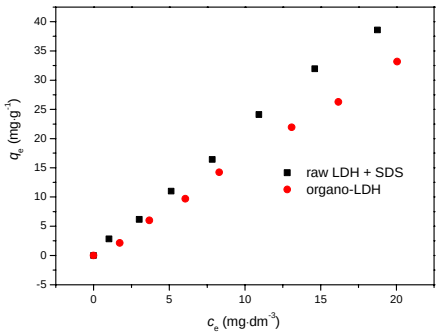

Fig. 4. Adsorption isotherms of DV28 on raw LDH-SDS.

The Langmuir adsorption isotherm is often used to describe adsorption of a solute from a liquid solution based on the assumption that the maximum adsorption corresponds to the saturated monolayer adsorption of adsorbate on specific homogeneous sites with a constant energy.[31] The isotherm can be represented as the following linear form:

$$\frac{c_e}{q_e} = \frac{1}{K_L q_m} + \frac{c_e}{q_m} \quad (2)$$

where c_e is the equilibrium concentration (mg·dm^{-3}), q_e the amount adsorbed at equilibrium (mg·g^{-1}) and q_m (mg·g^{-1}) and K_L (dm^3·mg^{-1}) are Langmuir constants related to adsorption capacity and energy of adsorption, respectively. A high K_L value indicates a higher affinity.

The Freundlich model is often used for nonideal adsorption on heterogeneous surfaces and multilayer adsorption.[32] It can be expressed by the following linear equation:

$$\log q_e = \log K_F + \frac{1}{n} \log c_e \quad (3)$$

where K_F (mg$^{1-1/n}$·dm$^{3/n}$·g^{-1}) is the Freundlich constant and $1/n$ (dimensionless) is the Freundlich exponent. K_F indicates the adsorption capacity. The magnitude of $1/n$ is an indicator of the favorability of adsorption. For beneficial adsorption, $1/n$ should lie between 1 and 0.1.[33]

The Linear adsorption isotherm, which is usually applied at low concentration of adsorbate, is often used to describe a partitioning adsorption mechanism,[34] and can be described simply as follows

$$q_e = K_d c_e + a \quad (4)$$

where K_d (dm^3·g^{-1}) is the distribution coefficient corresponding to the ratio of the amount (mg·g^{-1}) of the adsorbed chemical to its equilibrium aqueous concentration (mg·dm^{-3}), and a (mg·g^{-1}) is the linear regression constant. The higher K_d values correspond to a greater degree of adsorption.

The Temkin isotherm takes into account adsorbing species-adsorbent interactions. The isotherm assumes that: (i) the heat of adsorption decreases linearly with coverage due to adsorbent and adsorbate interactions; (ii) the adsorption is characterized by a uniform distribution of binding energies, up to some maximum binding energy.[35,36]

The Temkin isotherm is given as

$$q_e = \frac{RT}{b}\ln K_T + \frac{RT}{b}\ln c_e \quad (5)$$

where

$$B = \frac{RT}{b} \quad (6)$$

K_T is the equilibrium binding constant ($dm^3 \cdot mg^{-1}$) corresponding to the maximum binding energy and constant B is related to the heat of adsorption.

Another popular equation for the analysis of isotherm is that proposed by Dubinin and Radushkevich.[37] The Dubinin-Radushkevich equation can be cited to describe adsorption on both heterogeneous and homogeneous surfaces. Its linear form is:

$$\ln q_e = \ln q_s - B\varepsilon^2 \quad (7)$$

where q_s is the Dubinin-Radushkevich constant and ε can be correlated to temperature as:

$$\varepsilon = RT\ln\left(1+\frac{1}{c_e}\right) \quad (8)$$

where R is the gas constant (8.314 $J \cdot mol^{-1} \cdot K^{-1}$) and T is the absolute temperature (K). The constant B gives the mean free energy E of adsorption per molecule of the adsorbate when it is transferred to the surface of the adsorbent from infinity in the solution and can be computed using formula:

$$E = \frac{1}{\sqrt{2B}} \quad (9)$$

According to the Langmuir, Freundlich, Linear, Temkin, and Dubinin-Redushkevich isotherm equations, a detailed analysis of the adsorption equilibrium data of DV28 on raw LDH-SDS and organo-LDH at 293 K was done. The isotherm constants for all the isotherms studied, and the correlation coefficients R^2 with the experimental data are listed in Table 1.

Table 1

Langmuir, Freundlich, Linear, Temkin and Dubinin-Redushkevich isotherm constants for DV28 adsorption at 293 K.

Isotherm	Adsorbent	
	Organo-LDH	Raw LDH-SDS
Langmuir		
q_m (mg·g^{-1})	42.553	62.111
K_L (dm^3·mg^{-1})	0.029	0.045
R^2	0.982	0.971
Freundlich		
K_F (mg$^{1-1/n}$·dm$^{3/n}$·g^{-1})	1.307	2.606
$1/n$	0.927	1.095
R^2	0.984	0.986
Linear		
K_d (dm^3·kg^{-1})	1670	2087
R^2	0.999	0.997
Temkin		
B	12.371	12.209
K_T (dm^3·mg^{-1})	0.493	0.742
R^2	0.911	0.853
Dubinin-Redushkevich		
q_s (mg·g^{-1})	20.113	20.582
E (J·mol^{-1})	500	790
R^2	0.825	0.694

As seen from Table 1, the correlation coefficients for the Linear isotherm are highest in comparison to the values obtained for the Langmuir, Freundlich, Temkin, and Dubinin-Redushkevich isotherms. Therefore, the Linear isotherm is the best-fit isotherm for the adsorption of DV28 on raw LDH-SDS and organo-LDH. This finding indicated a partitioning adsorption mechanism at the studied concentration range: (1) in organo-LDH-DV28 system, DV28 was directly dissolved into the three-dimensional organic phase formed in organo-LDH layers; (2) in raw LDH-SDS-DV28 system, the self-assembly of SDS-LDH occurred, and then DV28 was dissolved into its organic interlayer regions. Additionally, the dissolution was unaffected by solution pH (Fig. 2) because of the weak polarity and difficult ionization of DV28 in these two systems. Table 1 showed that the degree of adsorption (K_d) for DV28 on raw LDH-SDS was higher than that on organo-LDH. This result indicated that cooperative removal and synergism between SDS and DV28 in solution occurred to a large extent during the one-step process. In addition, the organo-LDH surface was hydrophobic, which can cause organo-LDH powder to congregate and confer difficulty in wide dispersion, and DV28 molecules cannot easily permeate into the block. Accordingly, the amount of DV28 adsorbed by organo-LDH decreased.

The experimental data were also fitted to the Freundlich and Langmuir isotherms, although the fit

was not as good as the Linear isotherm. The higher value of K_F for raw LDH-SDS indicated it had a higher adsorption capacity for DV28. The value of $1/n$ lied between 1 and 0.1 for raw LDH-SDS, indicating that adsorption DV28 was favorable on it. The higher q_m (62.111 mg·g^{-1}) and K_L data for raw LDH-SDS also indicated that it showed higher adsorption capacity and higher affinity for DV28.

The Temkin and Dubinin-Redushkevich isotherm models did not exhibit good fit to the experimental equilibrium data as low correlation coefficient (R^2) values were observed for both raw LDH-SDS and organo-LDH.

3.4 Effect of temperature on DV28 removal

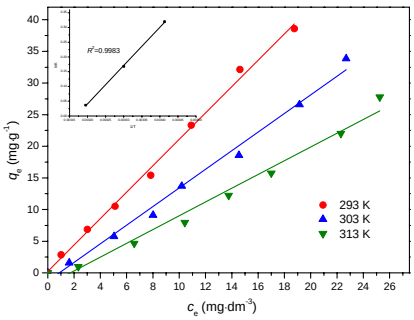

Fig. 5. Adsorption isotherms of DV28 on raw LDH-SDS at various temperatures (data dots refer to experimental result; solid lines refer to linear fitting result; inset is the plot of lnK_d VS. 1/T)

Table 2

Constants of the linear regression model based on DV28 adsorption isotherms at various temperatures.

Adsorbent	Temp. (K)	K_d (dm^3·kg^{-1})	R^2
Raw LDH-SDS	293	2087	0.997
Raw LDH-SDS	303	1472	0.991
Raw LDH-SDS	313	1087	0.982

Fig. 5 shows the equilibrium adsorption isotherms of DV28 on raw LDH-SDS at various temperatures. The equilibrium adsorption amount decreased with increased temperature, suggesting that interaction between DV28 and LDH was exothermic in nature. A comparison of experimental data with adsorption model fitting results showed that the linear equation gave the best fit of adsorption data ($R^2 > 0.98$) and that the distribution coefficient K_d decreased from 2087 to 1087 with increased temperature (Table 2).

Thermodynamic parameters such as Gibbs free energy (ΔG^o), standard enthalpy change (ΔH^o), and standard entropy change (ΔS^o) were determined using the following equations and van't Hoff plot:

$$\ln K_d = -\frac{\Delta H^o}{RT} + \frac{\Delta S^o}{R} \quad (10)$$

$$\Delta G^o = -RT \ln K_d = \Delta H^o - T\Delta S^o \quad (11)$$

where R is the universal gas constant (8.314 J·mol^{-1}·K^{-1}) and T is temperature (K). The values of ΔH^o (-10.70 kJ·mol^{-1}) and ΔS^o (-33.85 J·mol^{-1}·K^{-1}) were derived from the slope and intercept, respectively, of the van't Hoff plot (inset in Fig. 5). The negative values of ΔG^o (-772.87, -434.37, and -95 kJ·mol^{-1} at 293, 303, and 303 K, respectively) indicated that DV28 removal was a spontaneous process,[38] implying that the self-assembly of SDS-LDH was spontaneous and the hydrophobic force was sufficiently strong to break the potential and drive adsolubilization of DV28 into the hydrophobic interlayer region of the self-assembled SDS-LDH.

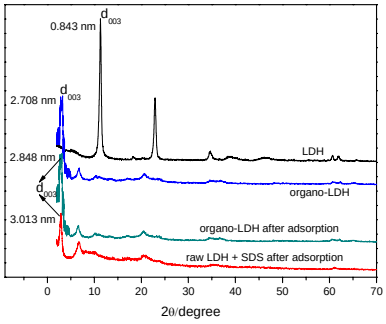

Fig. 6. PXRD patterns of adsorbents before and after adsorption.

PXRD patterns were used to further explain the adsorption mechanism and understand the structure of adsorbed LDH layer. In general, d_{003} represented the size of interlayer spacing of the samples. The d_{003} diffractions of raw LDH, organo-LDH, organo-LDH after adsorption, and raw LDH-SDS after adsorption were found at 2θ = 11.30, 3.26, 3.11, and 2.93, with distances of 0.843, 2.708, 2.848, and 3.013 nm, respectively (Fig. 6). The increased basal spacing values for organo-LDH can be attributed to the replacement of NO_3^- interlayer anions with $CH_3(CH_2)_{11}OSO_3^-$ anions.[34] d_{003} was positively correlated with the amount of adsorption on the adsorbent. Raw LDH-SDS showed a larger basal spacing than organo-LDH after adsorption, in accordance with the higher adsorption amount caused by the cooperative removal and synergism effect between SDS and DV28. In addition, when SDS was present in the one-step process, SDS was adsorbed onto both external and internal surface of LDH[34]: SDS adsorbed into the internal surface increased the interlayer space, and DV28 adsorption occurred within the interlayer through the interaction between DS^- and DV28; SDS adsorbed onto the external

surface can also attract more DV28 (Fig. 4).

3.5 Adsorption kinetics

The plots of removal rates of DV28 by raw LDH-SDS and organo-LDH against contact time at a constant initial concentration and 293 K are presented in Fig. 7. The kinetic equilibrium times required for raw LDH-SDS-DV28 and organo-LDH-DV28 system were almost 16 and 3 h, respectively. However, the equilibrium adsorption amount of raw LDH-SDS was about 38 mg·g^{-1}, higher than that of organo-LDH (about 33 mg·g^{-1}), which indicated the potential application of one-step process in a dyeing wastewater treatment system.

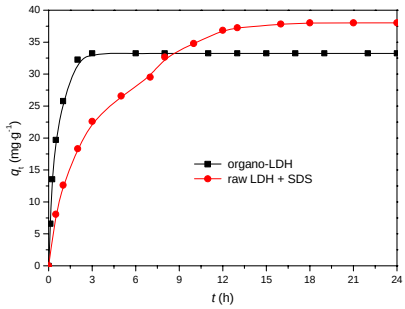

Fig. 7. Adsorption kinetics of DV28 on raw LDH-SDS and organo-LDH.

To study the various mechanisms underlying DV28 adsorption on raw LDH-SDS and organo-LDH, two kinetic models were tested.

Pseudo-first-order model[39] $$\ln(q_e - q_t) = \ln q_e - k_1 t \quad (12)$$

where q_t and q_e (mg·g^{-1}) are the amounts of DV28 adsorbed per unit mass of adsorbent at time t and at equilibrium, respectively. k_1 (min^{-1}) is the first-order rate constant of adsorption.

Pseudo-second-order model[40] $$\frac{t}{q_t} = \frac{1}{k_2 q_e^2} + \frac{1}{q_e} \cdot t \quad (13)$$

where k_2 (g·mg^{-1}·min^{-1}) is the second-order rate constant.

The conformity between experimental data and model-predicted values can be expressed by the correlation coefficient R^2. The calculated parameters and R^2 are listed in Table 3. For raw LDH-SDS, the pseudo-second-order model parameter, q_e, agreed well with the experimental value $q_{e,exp}$, with R^2 = 0.997. For organo-LDH, both R^2 of the pseudo-first-order and pseudo-second-order kinetic models were high, but the calculated q_e obtained from the pseudo-second-order kinetic equation did not agree well with the experimental value $q_{e,exp}$.

Table 3

Kinetic parameters for DV28 adsorption on raw LDH-SDS and organo-LDH at various temperatures.

Samples	Temp. (K)	$q_{e,exp}$ (mg·g^{-1})	Pseudo-first-order kinetics			Pseudo-second-order kinetics		
			k_1 (h^{-1})	q_e (mg·g^{-1})	R^2	k_2 (g·mg^{-1}·h^{-1})	q_e (mg·g^{-1})	R^2
Organo-LDH	293	33.26	1.72	33.20	0.990	0.047	39.68	0.997
Raw LDH-SDS	293	38.04	0.30	43.33	0.961	0.013	38.02	0.997
Raw LDH-SDS	303	33.10	0.20	20.73	0.947	0.023	33.22	0.994
Raw LDH-SDS	313	27.85	0.30	11.20	0.970	0.057	28.82	0.999

Two interactions occurred in the adsorption process of DV28 on raw LDH-SDS. Firstly, $CH_3(CH_2)_{11}OSO_3^-$ anions were intercalated into the interlayer of LDH, and NO_3^- ions were simultaneously released, as expressed by Eq. (1), which is the rate-limiting step. Secondly, DV28 was adsorbed into the interlayer of LDH. Ion exchange and adsorption simultaneously occurred in the one-step process. Ho et al.[41] suggested that the pseudo-second-order model, based on the assumption that the rate-limiting step may be chemisorption, provided the best correlation of data. Therefore, the process was controlled by chemisorption.

By contrast, only one interaction, the adsolubilization of DV28 in the hydrophobic interlayer regions of organo-LDH, occurred in the adsorption process of DV28 on organo-LDH. This step was quicker and controlled by physisorption, in accordance with the pseudo-first-order kinetic model.

3.6 Effect of temperature on the adsorption kinetics

Temperature is a highly significant parameter in adsorption. A series of experiments at different temperatures were performed to study the effect of temperature on the adsorption kinetics of DV28 on raw LDH-SDS. The results are shown in Fig. 8 and Table 3. Fig. 8 indicated that both the equilibrium adsorption amount and kinetic equilibrium time decreased with increased temperature. A comparison of experimental data with the adsorption kinetic model fitting results showed that the pseudo-second-order models represented the best fit of adsorption data (R^2 > 0.99) at different temperatures and the adsorption rate k_2 increased with increased temperature (Table 3). The adsorption rate constant k_2 may be described by the well-known Arrhenius equation:

$$\ln k_2 = -\frac{E_a}{RT} + C \quad (14)$$

where E_a (J·mol^{-1}) is the activation energy, R is the gas constant (8.314 J·mol^{-1}·K^{-1}), C is a constant, and T is the absolute temperature (K). The magnitude of activation energy provides information on

whether adsorption is mainly physical or chemical. Low activation energy values (5-40 kJ·mol^{-1}) are characteristic of physisorption, whereas higher values (40-800 kJ·mol^{-1}) suggest chemisorption.[42] The activation energy of adsorption (E_a) derived from the slope of the Arrhenius plot (inset in Fig. 8) was found to be 56.64 kJ·mol^{-1}, indicating that the process of DV28 removal was controlled by the rate of reassembly of SDS into LDH layer rather than by DV28 dissolution. Hence, the adsorption of DV28 on raw LDH-SDS was mainly a chemical process, in accordance with the results in section 3.5.

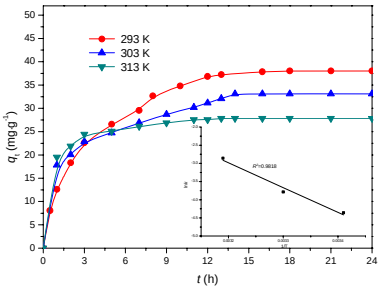

Fig. 8. Effect of temperature on the adsorption kinetics of DV28 on raw LDH-SDS (inset is the plot of lnk_2 VS. 1/T).

4. Conclusions

A one-step process for the simultaneous self-assembly of SDS-LDH and highly efficient removal of the non-ionic dye DV28 was realized. The adsorption process was found to be pH independent. Raw LDH-SDS showed better adsorption for DV28 than the traditional organo-LDH. The adsorption isotherm of DV28 on raw LDH-SDS fitted well with the Linear model, indicating a partitioning adsorption process. The adsorption kinetic data was well described by the pseudo-second-order model. PXRD analysis showed that raw LDH-SDS had a larger basal spacing than the traditional organo-LDH after adsorption. In the one-step process, SDS in wastewater was utilized to assemble with raw LDH and then used as an adsorbent to remove DV28, accompanied by the obvious interaction between DS^- and DV28. The high activation energy (56.64 kJ·mol^{-1}) indicated that the adsorption was mainly a chemical process. Thus, this simple one-step process involving both the self-assembly of SDS-LDH and the adsorption removal of non-ionic dyes was a low-cost, high-efficient, and promising method for treating dyeing wastewater.

Acknowledgements

This work was supported by the Natural Science Foundation of Shanxi Province of China

(2013011040-8), Scientific and Technological Innovation Programs of Higher Education Institutions in Shanxi (2013159), National Training Programs of Innovation and Entrepreneurship for Undergraduates (201310122002) and Training Programs of Innovation and Entrepreneurship for Undergraduates in Shanxi (2013358).

References

1 P. Wu, T. Wu, W. He, L. Sun, Y. Li and D. Sun, *Colloid Surface A*, 2013, **436**, 726-731.

2 Z. Aksu, A.I. Tatli and O. Tunc, *Chem. Eng. J.*, 2008, **142**, 23-39.

3 W.T. Tsai, C.Y. Chang, M.C. Lin, S.F. Chien, H.F. Sun and M.F. Hsieh, *Chemosphere*, 2001, **45**, 51-58.

4 I. Arslan and I.A. Balcioğlu, *Dyes Pigments*, 1999, **43**, 95-108.

5 K. Ravikumar, S. Ramalingam, S. Krishnan and K. Balu, *Dyes Pigments*, 2006, **70**, 18-26.

6 *Color chemistry – Synthesis, properties and applications of organic dyes and pigments*, ed. H. Zollinger,, V.C.H. Publishers, New York, 1991.

7 P.A. Carneiro, G.A. Umbuzeiro, D.P. Oliveira and M.V.B. Zanoni, *J Hazard Mater.*, 2010, **174**, 694-699.

8 S. Zodi, B. Merzouk, O. Potier, F. Lapicque and J.P. Leclerc, *Sep. Purif. Technol.*, 2013, **108**, 215-222.

9 G. Crini, *Bioresource Technol.*, 2006, **97**, 1061-1085.

10 Y.K. Ong, F Y. Li, S.P. Sun, B.W. Zhao, C.Z. Liang and T.S. Chung, *Chem. Eng. Sci.*, 2014, **114**, 51-57.

11 Y. Zhou, Z. Liang and Y. Wang, *Desalination*, 2008, **225**, 301-311.

12 V. David, G. G Vicente., E. Eduardo, A. Antonio and M. Vicente, *Sep. Purif. Technol.*, 2014, **123**, 15-22.

13 O. Türgay, G. Ersöz, S. Atalay, J. Forss and U. Welander, *Sep. Purif. Technol.*, 2011, **79**, 26-33.

14 B.E. Barragán, C. Costa and M.C. Márquez, *Dyes Pigments*, 2007, **75**, 73-81.

15 F.A. Batzias and D.K. Sidiras, *Bioresource Technol.*, 2007, **98**, 1208-1217.

16 Y. Kismir and A.Z. Aroguz, *Chem. Eng. J.*, 2011, **172**, 199-206.

17 P.K. Malik, *Dyes Pigments*, 2003, **56**, 239-249.

18 M. Toor and B. Jin, *Chem. Eng. J.*, 2012, **187**, 79-88.

19 G.Z. Kyzas, N.K. Lazaridis and M. Kostoglou, *Chem. Eng. Sci*., 2012, **81**, 220-230.

20 I. D. Mall, V.C. Srivastava and N.K. Agarwal, *Dyes Pigments*, 2006, **69**, 210-223.

21 N. Wang, D. O'Hare and J. Davis, *J. Mater. Chem.*, 2007, **17**, 2257-2266.

22 D.G. Evans and R.C.T. Slade, *Struct. Bond.*, 2006, **119**, 1-87.

23 F. Li and X. Duan, *Struct. Bond.*, 2006, **119**, 193-223.

24 M. Neamtu, A. Yediler, I. Siminiceanu, M. Macoveanu and A. Kettrup, *Dyes Pigments*, 2004, **60**, 61-68.

25 S. Carlino, *Solid State Ionics*, 1997, **98**, 73-84.

26 S.P. Newman and W. Jones, *New J. Chem.*, 1998, **22**, 105-115.

27 S. Miyata, *Clay Clay Miner.*, 1980, **28**, 50-56.

28 M.M. Saleh, *Water Res.*, 2006, **40**, 1052-1060.

29 D.Y. Yu, Y. Qiu and J. Zhang, *Chinese Journal of Analysis Laboratory*, 2010, **29(5)**, 13-16.

30 A. A. Atia, *Appl. Clay Sci*. 2008, **41**, 73-84.

31 I. Langmuir, *J Am. Chem. Soc*., 1918, **40**, 1361-1403.

32 H.M.F. Freundlich, *Zeitschrift fur Physikalische Chemie-Leipzig*, 1906, **57**, 385-470.

33 R. Sivaraj, C. Namasivayam and K. Kadirvelu, *Waste Manage.*, 2001, **21**, 105-110.

34 Y. You, H. Zhao and G.F. Vance, *Colloid Surface A*, 2002, **205**, 161-172.

35 M.I. Temkin and V. Pyzhev, *Acta Physiochimica URSS*, 1940, **12**, 327-356.

36 Y. Kim, C. Kim, I. Choi, S. Rengraj and J. Yi, *Environ. Sci. Technol.*, 2004, **38**, 924-931.

37 M.M. Dubinin and L.V. Raduskhevich, *Phys. Chem*., 1947, **55**, 327-329.

38 J.P. DiVincenzo and D.L. Sparks, *Arch. Environ. Contam. Toxicol.*, 2001, **40**, 445-450.

39 S. Lagergren, *K. Sven. Vetenskapsakad. Handl.*, 1898, **24**, 1-39.

40 Y.S. Ho and G. McKay, *Water Res.*, 2000, **34**, 735-742.

41 Y.S. Ho and G. McKay, *Process. Biochem.*, 1999, **34**, 451-465.

42 M. Doğan, M. Alkan, Ö. Demirbas¸ Y. Özdemir and C. Özmetin, *Chem. Eng. J.*, 2006, **124**, 89-101.

Table of Contents

Removal of disperse violet 28 from water using self-assembled organo-layered double hydroxides through a one-step process

Yan Li, Hao-Yu Bi, Yong-Sheng Jin and Xiao-Qin Shi

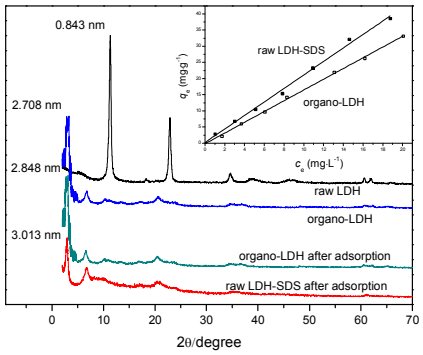

A simple one-step process involving the self-assembly of organo-LDH and the removal of non-ionic dyes from dyeing wastewater was realized.